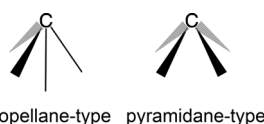


# Pentagermapyramidane: Crystallizing the “Transition-State” Structure\*\*

Vladimir Ya. Lee,\* Yuki Ito, Olga A. Gapurenko, Akira Sekiguchi,\* Vladimir I. Minkin,\*  
Ruslan M. Minyaev, and Heinz Gornitzka

**Abstract:** The first example of the homonuclear pyrimidanes, pentagermapyramidane, was synthesized, fully characterized, and computationally studied to reveal its peculiar structural features and the nature of its apex-to-base bonding interactions. Both solid-state and solution structures of pentagermapyramidane are discussed based on the computed stabilities of its square-pyramidal and distorted forms.

The classical theory of chemical bonding in organic chemistry is based on the tetrahedral geometry of the carbon atom, the revolutionary concept of van't Hoff and Le Bel that was proven to be true for the overwhelming majority of organic compounds.<sup>[1]</sup> The major reported departures from the classical tetrahedral nature of carbon are planarity and an “inverted” tetrahedral geometry at the carbon center, leading to changes both in its hybridization and in its bonding



**Scheme 1.** Inverted tetrahedral geometries at the carbon atom.

nature.<sup>[2]</sup> As shown in Scheme 1, the inverted stereochemistry at the carbon center may be of the propellane type<sup>[3]</sup> ( $C_{3v}$  symmetric with three bonds arranged about the central bond) or the pyramidane type<sup>[2,4,5]</sup> ( $C_{4v}$  symmetric with all four bonds symmetrically oriented about the central axis).

Although many propellanes, including the most synthetically challenging [1.1.1]propellanes, are known to be stable entities,<sup>[3]</sup> pyrimidanes were virtually unknown until very recently.<sup>[2,4,5]</sup> The first recognized examples of the pyrimidane family of the Group 14 elements, namely, germa- and stannapyrimidane derivatives, were reported by us recently.<sup>[6]</sup> However, all reported pyrimidanes have been heteronuclear, featuring different atoms at the apex (Ge or Sn) and in the base (C), causing a polarization of the apex-to-base bonds as a result of the natural difference in the electronegativity of Ge/Sn versus C atoms. The ideal model for structural studies of pyramidal compounds, in particular to study the nature of their nonclassical apex-to-base bonding interactions, is a homonuclear pyrimidane, in which apical and basal atoms are of the same type, thus causing minimal electronic perturbation to the system as a whole. However, the preparation of such homonuclear pyrimidanes is challenging when applying our previously reported synthetic strategy based on the reaction of the cyclobutadiene (CBD) dianion derivative and a Group 14 element dihalide.<sup>[6]</sup> For example, CBD dianion derivatives are synthetically accessible only as the carbon  $[(\text{Me}_3\text{Si})_4\text{C}_4]^{2-} \cdot 2\text{Li}^+$ ,<sup>[7]</sup> silicon  $[(t\text{Bu}_2\text{MeSi})_4\text{Si}_4]^{2-} \cdot [\text{K}^+(\text{thf})_2]_2$ ,<sup>[8]</sup> and germanium  $[(t\text{Bu}_2\text{MeSi})_4\text{Ge}_4]^{2-} \cdot [\text{K}^+(\text{thf})_2]_2$ <sup>[9]</sup> versions, whereas stable dihalides are available only in the case of germanium ( $\text{GeCl}_2 \cdot \text{diox}$ ;  $\text{diox} = 1,4\text{-dioxane}$ ), tin ( $\text{SnCl}_2 \cdot \text{diox}$  and  $\text{SnCl}_2$ ), and lead ( $\text{PbCl}_2$ ).<sup>[10]</sup> Thus, evidently the only synthetically available combination of identical apical and basal atoms is an all-germanium version, namely, the pentagermapyrimidane derivative  $\text{Ge}[\text{Ge}_4(\text{SiMe}_2\text{Bu}_2)_4]$  (**1**). The synthesis of this target compound, its structural characterization, and computational studies of its bonding situation are the focus of the present Communication.

As was anticipated, the target pentagermapyrimidane **1** was readily prepared by the straightforward reaction of the dioxane complex of dichlorogermylene  $\text{GeCl}_2 \cdot \text{diox}$ <sup>[11]</sup> with the dipotassium salt of the tetragermacyclobutadiene dianion  $\{[(t\text{Bu}_2\text{MeSi})_4\text{Ge}_4]^{2-} \cdot [\text{K}^+(\text{thf})_2]_2\}$ <sup>[9]</sup> (denoted  $2^{2-} \cdot [\text{K}^+(\text{thf})_2]_2$ ; Scheme 2).<sup>[12]</sup> Pentagermapyrimidane **1** showed only one set of resonance signals for all four  $t\text{Bu}_2\text{MeSi}$  substituents in the NMR spectra ( $^1\text{H}$ ,  $^{13}\text{C}$ ,  $^{29}\text{Si}$ ), indicative of its highly symmetrical composition in solution.

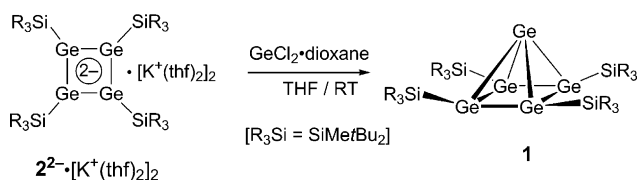
For structural and bonding insights, at the beginning we approached the problem from a computational viewpoint.<sup>[13]</sup>

[\*] Dr. V. Ya. Lee, Dr. Y. Ito, Prof. Dr. A. Sekiguchi  
Department of Chemistry  
Graduate School of Pure and Applied Sciences  
University of Tsukuba, 1-1-1 Tennodai  
Tsukuba 305-8571, Ibaraki (Japan)  
E-mail: leevya@chem.tsukuba.ac.jp  
sekiguch@chem.tsukuba.ac.jp

Dr. O. A. Gapurenko, Prof. Dr. V. I. Minkin, Prof. Dr. R. M. Minyaev  
Institute of Physical and Organic Chemistry  
Southern Federal University, 194/2 Stachki Ave.  
Rostov on Don 344090 (Russian Federation)  
E-mail: minkin@ipoc.sfedu.ru  
Prof. Dr. H. Gornitzka  
CNRS, LCC, Université de Toulouse, UPS, INPT  
205 route de Narbonne, BP 44099  
F-31077 Toulouse, Cedex 4 (France)

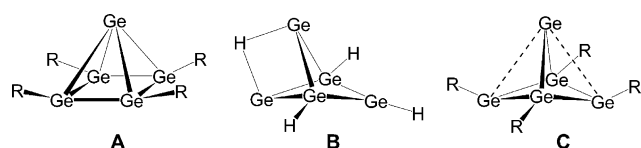
[\*\*] Financial support from the JSPS-RFBR Joint Japan–Russia Research Project, the Grant-in-Aid for Scientific Research program from the Ministry of Education, Science, Sports, and Culture of Japan (Nos. 23655027, 24245007, 24550038, and 90143164), and from the Russian Foundation for Basic Research (14-03-92101) and Russian Scientific Schools (NSC-274.2014.3) is gratefully acknowledged. R.M.M. thanks the Russian Ministry of Education and Science (project N4.71.2014/K).

Supporting information for this article is available on the WWW under <http://dx.doi.org/10.1002/anie.201500731>.



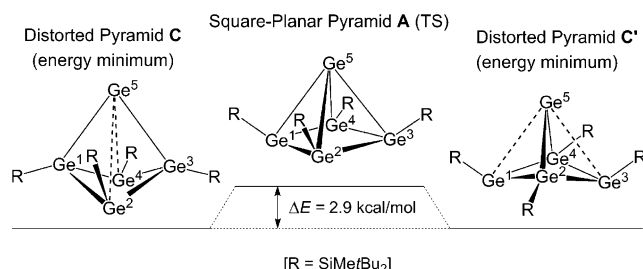
**Scheme 2.** Synthesis of the pentagermapyramidane **1**.

First, we found that the model compound  $Ge[Ge_4H_4]$ , with a planar pyramidal  $C_{4v}$ -symmetric structure **A** ( $R = H$ ), is the third-order saddle point on the  $Ge_5H_4$  potential energy surface (PES) with three imaginary frequencies ( $\lambda = 3$ ) at all levels of theory (likewise the analogous pyramidal  $Si[Si_4H_4]$  system) (Scheme 3).<sup>[14]</sup> The nearest local minimum is repre-



**Scheme 3.** Most representative structures of the  $Ge_5R_4$  PES: planar pyramidal **A**, hydrogen-bridged **B** ( $R = H$ ), and distorted pyramidal **C**.

sented by the H-bridged  $C_{2v}$ -symmetric structure **B** that is  $17.2 \text{ kcal mol}^{-1}$  (with zero-point energy (ZPE) corrections) more favorable than pyramidane **A**, whereas the folded pyramidal  $C_{2v}$ -symmetric structure **C** is a transition state (TS) of the permutational rearrangement that occurs between degenerate structures **B** (here and throughout the text we employed the B3LYP/6-311 + G\*\* level of theory) (Scheme 3). However, the relative stabilities of the planar pyramidal form **A** and folded pyramidal form **C** are finely balanced with the effect of substituents playing a decisive role (see Figure S1–S3 in the Supporting Information). Thus, the increase in the steric bulk of the substituents on going from the minimal H substituent to the substantially bigger  $H_3Si$  groups makes the folded pyramidal isomer **C** a local energy minimum (Table S1). Further increase in the size of substituents from  $H_3Si$  to  $Me_3Si$  and then to  $tBu_2MeSi$  groups stabilizes the planar pyramidal structure **A** as a TS, decreasing its energy gap with the local minimum **C** to as low as  $2.9 \text{ kcal mol}^{-1}$  (an even smaller value of  $2.3 \text{ kcal mol}^{-1}$  was obtained with the Def2TZVP basis set; Table S1). Thus, it was found that for the real compound  $Ge[Ge_4(SiMe(Bu)_2)_4]$  (**1**),



**Scheme 4.** Interconversion between the degenerate distorted pyramidal structures **C** and **C'** (energy minima) and square-planar pyramidal structure **A** (TS).

the conformational rearrangement of the folded pyramidal minima **C** through the planar pyramidal TS **A** proceeds with an exceptionally low inversion barrier (Scheme 4). These calculations can explain the fact that only one set of NMR resonance signals were detected for **1**, caused by the smooth and fast ( $Ge_1-Ge_2-Ge_3-Ge_4$ )-base flipping on the NMR timescale, resulting in an averaging of the signals.

Most strikingly, this theoretical prediction was corroborated by the results of the characterization of pentagermapyramidane **1** by X-ray crystallography. Upon crystallization of **1**, two distinct sets of single crystals were isolated (both crystallizing in the same  $P\bar{1}$  space group), that manifested remarkably different geometries of their  $Ge_4$  bases.<sup>[12]</sup> In the first set of crystals (**1a**; Figure 1a), the  $Ge_4$  base is notably

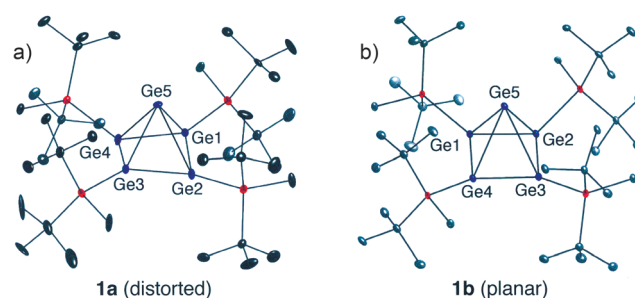
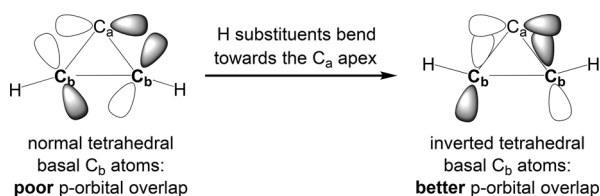


**Figure 1.** Crystal structures of two structural variations of pentagermapyramidane **1**: a) **1a** with the distorted  $Ge_1-Ge_2-Ge_3-Ge_4$  base and b) **1b** with the planar  $Ge_1-Ge_2-Ge_3-Ge_4$  base. ORTEP representations are shown and thermal ellipsoids are set at 40% probability. Only the main positions of both disordered structures are depicted for clarity.

distorted ( $Ge_4$  ring-folding angles are  $17.59^\circ$  and  $17.69^\circ$ ) and accordingly the  $Ge_5$  apex features two shorter bonds to the  $Ge_4$  base ( $Ge_5-Ge_1$   $2.546(5) \text{ \AA}$ ,  $Ge_5-Ge_3$   $2.514(4) \text{ \AA}$ ; calculated value  $2.54 \text{ \AA}$ ) and two longer bonds ( $Ge_5-Ge_2$   $2.707(8) \text{ \AA}$ ,  $Ge_5-Ge_4$   $2.765(5) \text{ \AA}$ ; calculated value  $2.98 \text{ \AA}$ ). In contrast, in the second set of crystals **1b**, the  $Ge_4$  base is planar with negligible folding of  $0.09^\circ$  and the  $Ge_5$  apex is evenly perhaptoordinated to the base, which overall constitutes a regular square-pyramidal shape (Figure 1b). Both **1a** and **1b** showed disorder of the molecule with occupancy ratios of 51/49 (**1a**) and 56/41/3 (**1b**), respectively. To ensure that our assignment of the different disordered groups is reliable for both structures **1a** and **1b**, the occupancies of all Ge and Si atoms were refined independently.

The origin of the skeletal disorder in both cases is the slight shift of the whole molecule along the vertical axis running through the apical Ge atom and the center of the  $Ge_4$  base. Although disorder in **1a** and **1b** precludes accurate discussion of their metric parameters, it should be emphasized that the  $Ge-Ge$  bond lengths within the  $Ge_4$  base in both conformations range from  $2.327(2)$  to  $2.399(4) \text{ \AA}$  (calculated values  $2.41-2.46 \text{ \AA}$ ), and are thus intermediate between the sum of the single-bond covalent radii of the Ge atoms ( $2.42 \text{ \AA}$ )<sup>[15]</sup> and the sum of their double-bond covalent radii ( $2.22 \text{ \AA}$ ).<sup>[16]</sup> This intermediacy in  $Ge-Ge$  bond lengths within the  $Ge_4$  base implies cyclic electron delocalization.<sup>[17]</sup> In contrast, in **1b** the apex-to-base  $Ge-Ge$  bonds are notably

longer than the basal Ge–Ge bonds, ranging from 2.797(7) to 2.873(7) Å (calculated value 2.72 Å). Remarkably, in the planar pentagermapyramidane **1b**, all four silyl substituents are bent towards the germanium apex Ge5 (Figure 1). This structure can be considered as the first experimental verification of that theoretically predicted for the all-carbon analogue  $C[C_4H_4]$  to compensate for the decreased  $P_{\text{(basal C)}}-P_{\text{(apical C)}}$  bonding orbital overlap (Scheme 5).<sup>[18]</sup> Thus, **1b** represents a puzzling structure, experimentally realized for the first time, in which all skeletal atoms have inverted tetrahedral geometry.



**Scheme 5.** Orbital interaction in the normal tetrahedral (left) and inverted tetrahedral (right) geometries of the parent pyramidane  $C[C_4H_4]$ .

Overall, the structure of the distorted pyramidal isomer **1a** (Figure 1) corresponds to the computationally established energy-minimized structures **C** and **C'** (Scheme 4), whereas the planar pyramidal form **1b** (Figure 1) represents a “frozen” TS **A** on the  $Ge_5R_4$  PES (Scheme 4). Isolation of the planar pyramidal structure **1b** is therefore of particular importance, given the commonly accepted view of the “transition state” as the hypothetical local-energy maximum along the reaction coordinate on the way from the substrate to the product, that typically cannot be isolated as an individual compound.<sup>[19]</sup> Definitely, crystallization of the transition state **A** in the form of **1b** was enabled by the exceptionally low inversion barrier theoretically predicted for the folded pyramidal structure **C** (Scheme 4).<sup>[20]</sup>

Atoms-in-molecules (AIM) topological analysis<sup>[13]</sup> clearly demonstrated the presence of the bonding paths between the basal and apical Ge atoms in the model compound  $Ge[Ge_4H_4]$  (Figure S4). Importantly, although the values of the electron density  $\rho(r)$  are relatively small for the basal Ge–Ge bonds, the negative values of the Laplacian of the electron density  $\nabla^2\rho(r)$  point to their predominantly covalent nature (Table S2). Classification of the pyramidal Ge–Ge bonds between the apical and basal Ge atoms is not that straightforward because of the positive values of  $\nabla^2\rho(r)$ . However, these bonds can be qualified as homopolar covalent bonds (intermediate interaction; Table S2) because of the negative values of the local electron energy  $h_e(r)$  ( $h_e(r) < 0$  for covalent bonding<sup>[21,22]</sup>) that is defined by the equation  $h_e(r) = v(r) + g(r)$ ,<sup>[22,23]</sup> where  $v(r)$  and  $g(r)$  are the local potential and kinetic-energy densities, respectively.

Overall, in contrast to the heteronuclear germa- and stannapyramidanes  $E[C_4(SiMe_3)_4]$  ( $E = Ge, Sn$ ),<sup>[6]</sup> for which the ionic form is of crucial importance as a result of the high E–C bond polarity, the contribution of the ionic resonance form ( $[tBu_2MeSi)_4Ge_4]^{2-} \rightarrow Ge^{2+}$ ) is less important for the

homonuclear pentagermapyramidane **1**. In accord with such a conclusion, **1b** shows a negligible natural charge separation within the molecule (−0.11 for the apical Ge atom and −0.15 for each of the basal Ge atoms), whereas in germapyramidane  $Ge[C_4(SiMe_3)_4]$  the charge separation was substantially greater (natural charges are +0.69 for the apical Ge atom and −0.65 for each of the basal C atoms)<sup>[6]</sup>. Furthermore, according to the natural bond orbital (NBO) analysis, the pyramidal Ge–Ge bonds in **1b** are insignificantly polar (polarization coefficients are 0.59 and 0.41 for the basal and apical Ge atoms, respectively), whereas in  $Ge[C_4(SiMe_3)_4]$  the pyramidal Ge–C bonds are remarkably polarized towards the basal C atoms (polarization coefficients are 0.75 and 0.25 for the basal C and apical Ge atoms, respectively).

Considering the electron localization function (ELF) topological analysis,<sup>[13]</sup> two features can be identified: a) the presence of the lone pair with very high s character (87 % for **1b** by NBO analysis) at the apical Ge atom and b) remarkably weaker pyramidal Ge–Ge bonds compared with the basal Ge–Ge bonds (Table S3, Figure S5). Even more so, the basin population  $N$  for the pyramidal Ge–Ge bonds progressively increases (from 0.77 to 0.91) with increasing steric bulk of the substituents from H to  $tBu_2MeSi$  groups (Table S3). This is in line with the above-drawn conclusion that the larger substituents better stabilize the planar pyramidal shape.

The molecular orbital (MO) interaction diagram (Figure 2) clearly shows the presence of a lone pair at the Ge apex seen in the HOMO-2 ( $4a_1$ ; HOMO = highest occupied molecular orbital) and stabilizing bonding interactions resulting from the formation of the doubly-degenerate HOMO and HOMO-1 ( $3e$ ). Inspection of the lower-energy orbital  $2a_1$  shows the bonding interaction between the apex and base. However, the extent of this interaction is notably

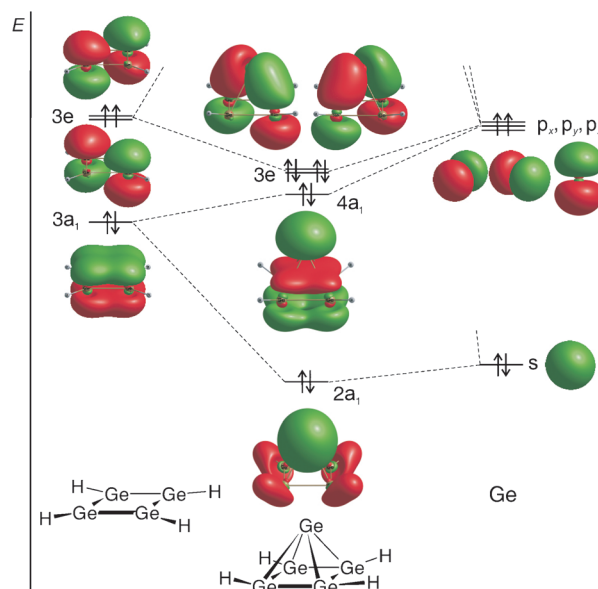


**Figure 2.** Schematic MO interaction diagram showing the formation of the principal orbitals from fragment orbitals, as computed at the B3LYP/6-311 + G\*\* level of theory for the parent pentagermapyramidane  $Ge[Ge_4H_4]$ . Only bonding interactions are shown.

smaller than in the case of the previously reported all-carbon pyramidane  $C[C_4H_4]$ , thus leading to weaker Ge–Ge pyramidal bonds in pentagermapyramidane, compared with their C–C congeners in all-carbon pyramidane. This can be seen by comparison of the values of the Wiberg bond indices (WBI) for pentagermapyramidane **1b** and carbon pyramidane  $C[C_4H_4]$ : 0.66 versus 0.70 (for the pyramidal bonds) and 1.01 versus 1.10 (for the basal bonds).

Overall, in this study we present the first example of a homonuclear pyramidane, the pentagermapyramidane derivative **1**. The peculiar structural and bonding features of **1** are studied both experimentally and computationally to show its particular nature as a nonclassical polyhedral compound.

**Keywords:** cage compounds · density functional calculations · germanium · NMR spectroscopy · X-ray diffraction

**How to cite:** *Angew. Chem. Int. Ed.* **2015**, *54*, 5654–5657  
*Angew. Chem.* **2015**, *127*, 5746–5749

- [1] a) J. H. van't Hoff, *Arch. Neerl. Sci. Exactes Nat.* **1874**, *9*, 445; b) J.-A. Le Bell, *Bull. Soc. Chim. Fr.* **1874**, *22*, 337.
- [2] For reviews, see: a) V. I. Minkin, R. M. Minyaev, R. Hoffmann, *Russ. Chem. Rev.* **2002**, *71*, 869; b) V. I. Minkin, *Russ. Chem. Bull. Int. Ed.* **2012**, *61*, 1265.
- [3] For reviews, see: a) K. B. Wiberg, *Chem. Rev.* **1989**, *89*, 975; b) M. D. Levin, P. Kaszynski, J. Michl, *Chem. Rev.* **2000**, *100*, 169.
- [4] For theoretical studies, see: a) V. I. Minkin, R. M. Minyaev, G. V. Orlova, *J. Mol. Struct. (Theochem)* **1984**, *110*, 241. See also: b) V. I. Minkin, R. M. Minyaev, Yu. A. Zhdanov, *Nonclassical Structures of Organic Compounds*, Mir Publishers, Moscow, **1987**; c) E. Lewars, *J. Mol. Struct. (Theochem)* **1998**, *423*, 173; d) E. Lewars, *J. Mol. Struct. (Theochem)* **2000**, *507*, 165; e) J. P. Kenny, K. M. Krueger, J. C. Rienstra-Kiracofe, H. F. Schaefer III, *J. Phys. Chem. A* **2001**, *105*, 7745.
- [5] For early calculations on pyramidal structures, see: a) V. I. Minkin, R. M. Minyaev, I. I. Zacharov, *J. Chem. Soc. Chem. Commun.* **1977**, 213; b) V. I. Minkin, R. M. Minyaev, I. I. Zacharov, V. I. Avdeev, *Zh. Org. Khim.* **1978**, *14*, 3 (*Russ. J. Org. Chem.*).
- [6] V. Ya. Lee, Y. Ito, A. Sekiguchi, H. Gornitzka, O. A. Gapurenko, V. I. Minkin, R. M. Minyaev, *J. Am. Chem. Soc.* **2013**, *135*, 8794.
- [7] A. Sekiguchi, T. Matsuo, H. Watanabe, *J. Am. Chem. Soc.* **2000**, *122*, 5652.
- [8] V. Ya. Lee, K. Takanashi, T. Matsuno, M. Ichinohe, A. Sekiguchi, *J. Am. Chem. Soc.* **2004**, *126*, 4758.
- [9] V. Ya. Lee, Y. Ito, H. Yasuda, K. Takanashi, A. Sekiguchi, *J. Am. Chem. Soc.* **2011**, *133*, 5103.
- [10] Synthetically available  $SiCl_2$ –NHC (NHC = N-heterocyclic carbene) complex [R. S. Ghadwal, H. W. Roesky, S. Merkel, J. Henn, D. Stalke, *Angew. Chem. Int. Ed.* **2009**, *48*, 5683; *Angew. Chem.* **2009**, *121*, 5793], exhibiting a rather strong donor–acceptor interaction between the NHC and dichlorosilylene units, in many cases behaves differently compared with the dioxane complexes of  $GeCl_2$  and  $SnCl_2$  featuring loosely bound coordination to dioxane.
- [11] S. P. Kolesnikov, I. S. Rogozhin, O. M. Nefedov, *Izv. Akad. Nauk SSSR Ser. Khim.* **1974**, 2379 [English translation: *Bull. Acad. Sci. USSR, Div. Chem. Sci.* **1974**, 2297].
- [12] Experimental details for the synthesis of pentagermapyramidane **1** and spectroscopic and crystallographic data (for both **1a** and **1b**) are given in the Supporting Information. CCDC-1044815 (**1a**) and 1044816 (**1b**) contain the supplementary crystallographic data for this paper. These data can be obtained free of charge from The Cambridge Crystallographic Data Centre via [www.ccdc.cam.ac.uk/data\\_request/cif](http://www.ccdc.cam.ac.uk/data_request/cif).
- [13] Computations were performed with the Gaussian09 program at the DFT B3LYP and ab initio CCSD levels with the 6-311 + G(d,p) and Def2TZVP basis sets. References for these computational methods, as well as on the AIM and ELF topological analyses, and full reference on the Gaussian 09 program and other programs, are given in the Supporting Information.
- [14] O. A. Gapurenko, R. M. Minyaev, V. I. Minkin, *Mendeleev Commun.* **2012**, *22*, 8.
- [15] P. Pyykkö, M. Atsumi, *Chem. Eur. J.* **2009**, *15*, 186.
- [16] P. Pyykkö, M. Atsumi, *Chem. Eur. J.* **2009**, *15*, 12770.
- [17] The cyclic electron delocalization in **1a** and **1b** is clearly visualized in the HOMO-2 ( $4a_1$ ; Figure 2) and is further supported by the nucleus-independent chemical shift (NICS) calculation: NICS(1) = –14.7 (for **1a**) and –15.1 (for **1b**).
- [18] V. I. Minkin, R. M. Minyaev, *Doklady Chemistry* **2002**, *385*, 203.
- [19] For isolable TS-like structures, see: a) K. Akiba, M. Yamashita, Y. Yamamoto, S. Nagase, *J. Am. Chem. Soc.* **1999**, *121*, 10644; b) M. Yamashita, Y. Yamamoto, K. Akiba, D. Hashizume, F. Iwasaki, N. Takagi, S. Nagase, *J. Am. Chem. Soc.* **2005**, *127*, 4354; c) H. Hashimoto, Y. Odagiri, Y. Yamada, N. Takagi, S. Sakaki, H. Tobita, *J. Am. Chem. Soc.* **2015**, *137*, 158.
- [20] Given the shallow  $Ge_5R_4$  PES (Scheme 4), it is likely that the observed structural changes (i.e. from **1a** to **1b**) are driven by small changes in the environment, such as crystal-packing effects.
- [21] R. F. W. Bader, H. Essén, *J. Chem. Phys.* **1984**, *80*, 1943.
- [22] D. Cremer, E. Kraka, *Croat. Chem. Acta* **1984**, *57*, 1259.
- [23] a) D. Cremer, E. Kraka, *Angew. Chem. Int. Ed. Engl.* **1984**, *23*, 627; *Angew. Chem.* **1984**, *96*, 612; b) R. F. W. Bader, *J. Phys. Chem. A* **1998**, *102*, 7314.

Received: January 29, 2015

Revised: February 18, 2015

Published online: March 13, 2015